https://doi.org/10.55415/deep-2023-0056.v1

Structure-based virtual screening for novel p38MAPK inhibitors and their biological evaluation

Qinwen Zheng[1,#], Yumeng Zhu[1, #], Aoxue Wang[1, #], Panpan Yang[1], Xin Wang[1], Wen Shuai[1, *], Liang Ouyang[1, *], Guan Wang[1,*]

[1] Department of Biotherapy, Cancer Center and State Key Laboratory of Biotherapy, Innovation Center of Nursing Research, Nursing Key Laboratory of Sichuan Province, West China Hospital, Sichuan University /West China School of Nursing, Sichuan University, Chengdu 610041, China

[#] These authors made equal contributions to this work.

* Correspondence: shuaiwen05@163.com (W. S.), ouyangliang@scu.edu.cn (L. O.), guan8079@163.com (G. W.)

Abstract: Mitogen-activated protein kinases (MAPK) are a group of serine-threonine protein kinases that can be activated by extracellular stimuli. p38α(MAPK14) affects major disease processes, inhibition of p38α has been shown to have potential therapeutic effects. Many inhibitors targeting p38α have entered clinical trials but have a long development cycle and serious side effects. We developed a multi-step receptor structure-based virtual screening method to screen potential bioactive molecules from SPECS and our libraries of MCDB. Compound **10** was identified as a promising p38α inhibitor, which may be used in the treatment of p38αMAPK pathway-related diseases, but further exploration is needed.

Keywords: P38α; Inhibitors; Virtual screening; Activity test

1. Introduction

P38MAPK was discovered in 1993 while studying the effect of hypertonic environment on fungi. It was first considered to be a stress-activated protein kinase like JNK. In recent years, it has been found that p38MAPK plays a role in a variety of tumors, and related studies have emerged. P38MAPK have four isoforms, including p38α (MAPK14), p38β (MAPK11), p38γ (MAPK12) and p38δ (MAPK13). The distribution of the four isoforms is also tissue specific. P38α and p38β are widely present in various tissue cells, p38γ is only present in skeletal muscle cells, and p38δ

is mainly present in glandular tissues.

P38MAPK has a close relationship with cancer. In normal physiological activities, p38MAPK is related to cell cycle, differentiation, metabolism, senescence, and other cellular processes. For example, Whitaker et al. [1] demonstrated that p38 affects G1 and G2 phases in the cell cycle. Weng et al. [2] proved that amiodarone regulates cell proliferation and myofibroblast differentiation in human embryonic lungfibroblasts (HELF) by regulating the p38MAPK pathway, while cancer cells can destroy the pathway to promote proliferation, survival, and invasion. The p38MAPK pathway regulates cell cycle progression and cellular programs for cell survival and differentiation at different transition points through transcription-dependent mechanisms [3], which contributes to its impact on a variety of cancers. In many cancer cells such as liver cancer and lung cancer, the activation of p38α is usually associated with anti-proliferative function. And p38α negatively regulates the abnormal proliferation of various types of primary cells, including cardiomyocytes, hepatocytes, fibroblasts, hematopoietic cells, and lung cells [4-6]. P38α can also promote apoptosis in some cells. In the early transformation process, reactive oxygen species (ROS) can induce the activation of p38α to induce cell apoptosis, thereby preventing the carcinogenic effect caused by the accumulation of reactive oxygen species [7]. P38α also mediates cell survival through a quiescent state named cancer quiescence, which is important for cancer cell resistance. P38α is associated with the G2/M checkpoint, which induces cell cycle arrest and promotes DNA repair, possibly leading to apoptotic resistance of cancer cells [8]. Therefore, developing inhibitors targeting p38α, which is the most widely distributed and influential p38 isoforms, is a priority.

Computer-aided drug design (CADD) is considered to have changed the traditional drug design industry in recent years. It consists of two technologies: structure-based drug design (SBDD) and ligand-based drug design (LBDD), which are considered to show good accuracy in the field of developing drug lead molecules [9]. SBDD has also been recognized as an optimal method to generate and optimize ligands for the pharmaceutical industry [10]. The basic steps of SBDD are further divided into target preparation, binding site identification, molecular docking, virtual screening, and molecular dynamics. Among them, structure-based virtual screening (SBVS) is used to screen novel bioactive compounds against specific therapeutic targets from various compound libraries in early drug development projects. In addition to predicting

binding modes, SBVS also ranks the docked molecules by docking scores. This rating can be used as the sole criterion for select out hits. Moreover, it can be combined with other evaluation methods, such as combining with biological assays to determine the biological activity of hits against the molecular target under study [11].

Herein, we used a structure-based virtual screening approach to screen lead compounds inhibiting p38α from compounds libraries established by ourselves via multiple screening process. Among them, compound **10** showed potential inhibitory activity against p38α, which deserve as a promising lead compound for further investigation.

2. Results and Discussion

2.1 Structure-based virtual screening

The most significant advantage of structure-based virtual screening can efficiently identify novel chemical structures against targets of interest from large chemical libraries. To improve more precisely the selectivity of p38α inhibitors, key residues in the p38α binding pocket were analyzed. From analyzing all co-crystal structures contained in the protein data bank (PDB), Asp168, Glu71, and Met109 are key amino acid residues in the interaction (Figure 1). Subsequently, multiple docking was performed in the Discovery Studio program to screen selective p38α inhibitors.

https://doi.org/10.55415/deep-2023-0056.v1

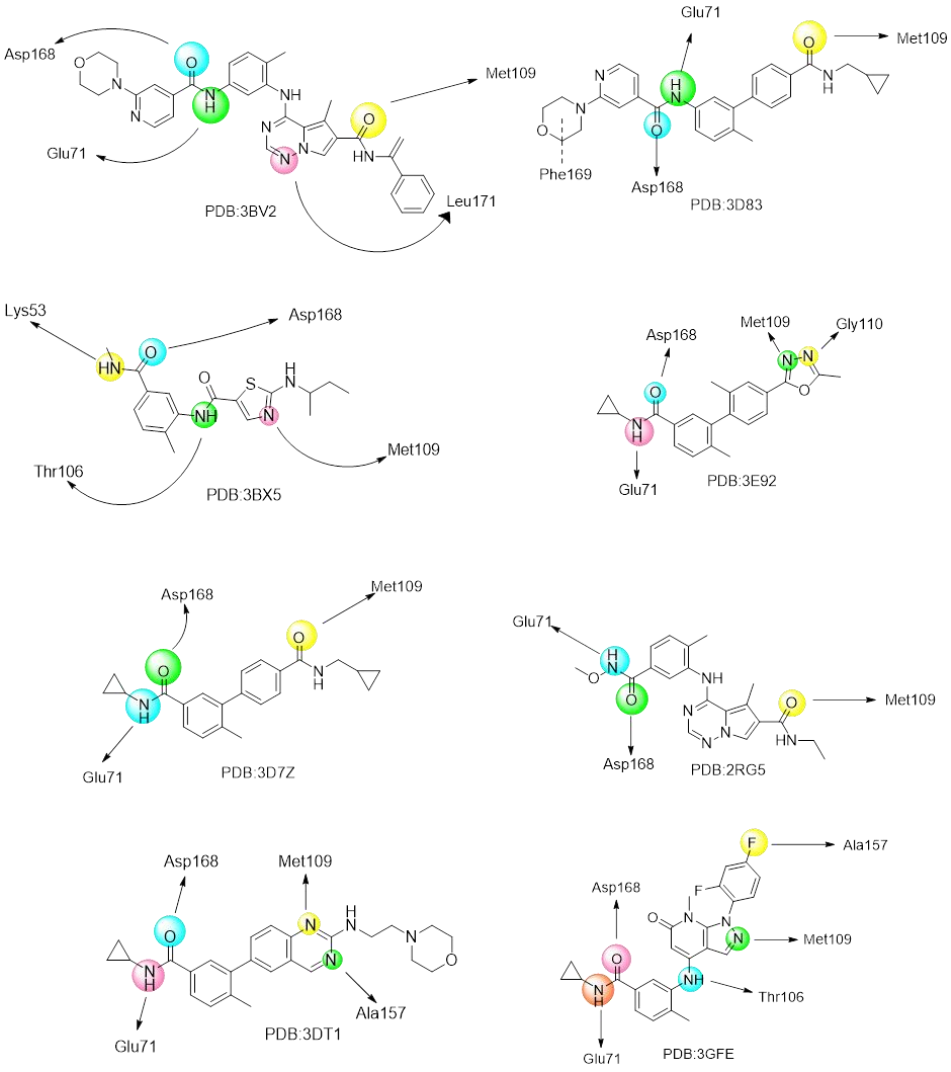

Figure 1. The intermolecular forces and important amino acid residues of the existing inhibitors interacting with p38α.

Firstly, The Lipinski's rule of five were used to screen more than 200,000 compounds in the MCDB library established by our laboratory and the SPECS library. In this study, a total of 196,432 small-molecule compounds were obtained for the following docking-based virtual screening.

Next, these molecules were scored by docking analysis using the co-crystal structure of human p38αMAPK (PDB code: 1A9U) through the LibDock module in the Discovery Studio software. The top 1000 molecules with scores between 121.995 and 153.925 were selected for the second screening. The CDOCKER module was further used to analyze the 1000 screening results of p38α more accurately. And the CDOCKER-energy score was obtained to screen out 10 molecules with a score above

https://doi.org/10.55415/deep-2023-0056.v1

17.6255 as candidates for further analysis. Finally, 10 candidate p38αMAPK inhibitors were identified by visual inspection of the selected library, including evaluation of shape complementarity, hydrogen bonds, hydrophobic contacts, binding pattern similarity, specific ligand-protein interactions, and docking scores, taking into consideration the diversity of molecular frameworks (Table 1). It is convenient for the subsequent test of inhibition ability.

Table 1. Virtual Screening Results.

No.	Structure	Chemical name	-CDOCKER ENERGY	LibDock Score
1	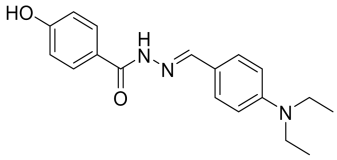	DY131	35.2763	122.036
2	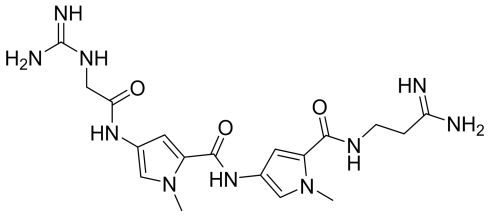	Netropsin (dihydrochloride)	52.0194	148.964
3	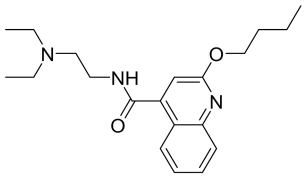	Dibucaine (hydrochloride)	17.6255	121.995
4	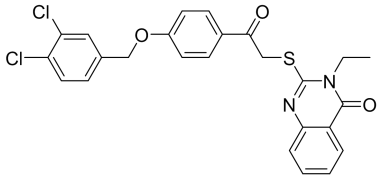	2-[(2-4-[(3,4-dichlorobenzyl)oxy]phenyl -2-oxoethyl)sulfanyl]-3-ethyl-4(3H)-quinazolinone	36.5970	153.925
5	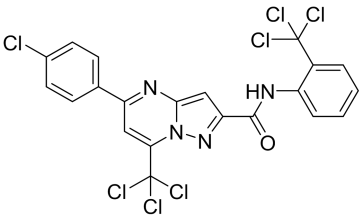	5-(4-chlorophenyl)-7-(trifluoromethyl)-N-[2-(trifluoromethyl)phenyl]pyrazolo[1,5-a]pyrimidine-2-carboxamide	29.8581	125.353
6	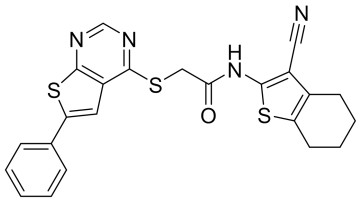	N-(3-cyano-4,5,6,7-tetrahydro-1-benzothien-2-yl)-2-[(6-phenylthieno[2,3-d]pyrimidin-4-yl)sulfanyl]acetamide	29.3654	145.929
7	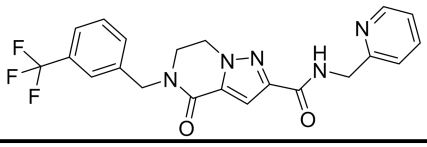	4-oxo-N-[(pyridin-2-yl)methyl]-5- [3-(trifluoromethyl)phenyl]methyl-4H,5H,6H,7H-	37.0194	146.836

https://doi.org/10.55415/deep-2023-0056.v1

		pyrazolo[1,5-a]pyrazine-2-carb		
8	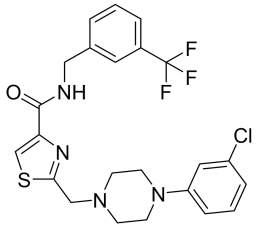	2-[4-(3-chlorophenyl)piperazin-1-yl]methyl-N-[3-(trifluoromethyl)phenyl]methyl-1,3-thiazole-4-carboxamide	40.4858	140.802
9	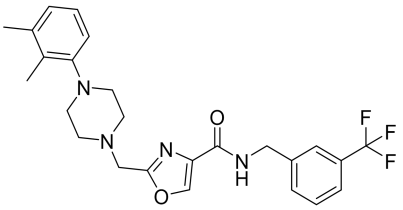	2-[4-(2,3-dimethylphenyl)piperazin-1-yl]methyl-N-[3-(trifluoromethyl)phenyl]methyl-1,3-oxazole-4-carboxamid	42.0744	142.277
10	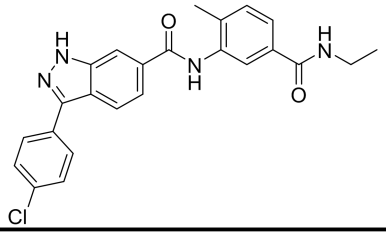	3-(4-chlorophenyl)-N-(5-(ethylcarbamoyl)-2-methylphenyl)-1H-indazole-6-carboxamide	33.8025	137.116

2.2 P38α kinase inhibitory assays

The luminescence signal was detected by the multifunctional microplate reader used in the ADP-GloTM luminescence method, which was converted into the corresponding amount of ATP consumed to judge the cell activity. The IC_{50} was obtained after fitting the curve. 10 compounds were measured separately and the IC_{50} is listed as follows. Among the 10 compounds, compound **10** showed the best inhibitory effect against p38α, with an IC_{50} value of 3.37 ± 0.24 μM.

2.3 Cell viability assay

J.w. Altoon et al. demonstrated that RWJ67657, a p38α inhibitor, effectively inhibited the p38 pathway in MDA-MB-361 breast cancer cells and inhibited the growth of endocrine-resistant breast cancer tumors *in vitro* and *in vivo* [12]. Our laboratory is committed to the development of inhibitors for triple negative breast cancer in the long term. Therefore, MDA-MB-231 and MDA-MB-468, two triple negative breast cancer cells, were selected for cell anti-proliferation experiments. MTT assay was used to compare the number of surviving cells to obtain the cell inhibition rate under different concentration gradients. The IC_{50} value of each compound was calculated against two triple-negative breast cancer cells (Table 2).

https://doi.org/10.55415/deep-2023-0056.v1

The results showed that compound **10** not only showed an inhibitory activity in the kinase assay (IC_{50} = 3.37 ± 0.24 μM), but also had a potent anti-proliferative effect on MDA-MB-231 and MDA-MB-468 cancer cells with IC_{50} values of 8.21 ± 1.24 μM and 10.08 ± 2.11 μM respectively (Figure 2). In contrast, the other 9 compounds obtained by screening were slightly lower activity.

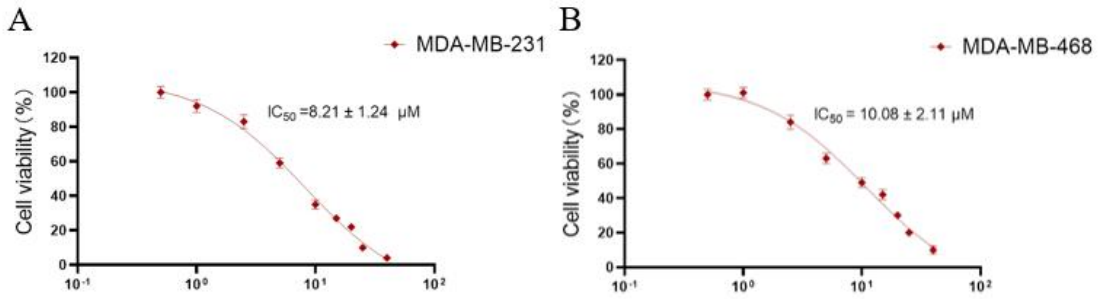

Figure 2. (A, B) Inhibition rate-concentration curves of compound **10** on MDA-MB-231 and MDA-MB-468.

Table 2. The inhibitory activities of 10 compounds against p38α, MDA-MB-231 and MDA-MB-468.

No.	Structure	p38α (IC_{50}, μM)	Anti-proliferative activity (IC_{50}, μM)	
			MDA-MB-231	MDA-MB-468
1	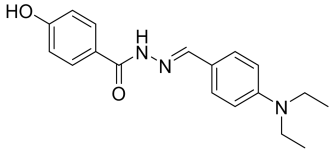	6.23 ± 1.01	19.21 ± 2.18	12.60 ± 3.02
2	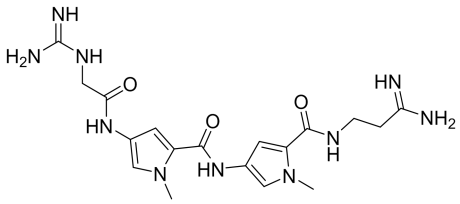	9.06 ± 3.25	15.56 ± 1.25	17.21 ± 3.88
3	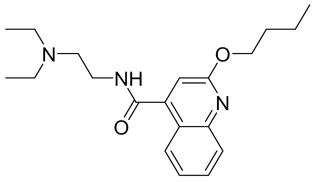	5.91 ± 0.31	9.36 ± 1.25	13.88 ± 2.08
4	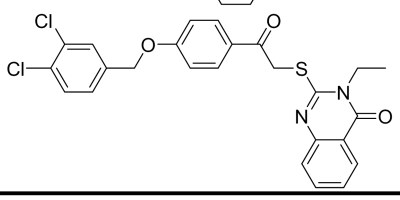	7.70 ± 1.23	9.41 ± 1.34	12.40 ± 3.96

https://doi.org/10.55415/deep-2023-0056.v1

5	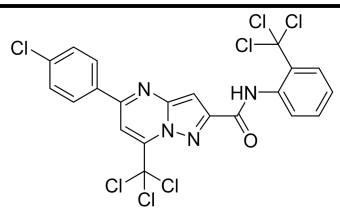	5.82 ± 0.71	15.12 ± 1.05	15.89 ± 3.11
6	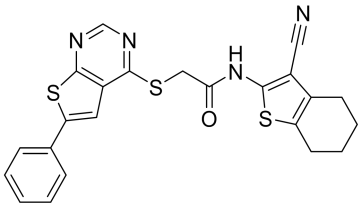	6.96 ± 0.91	20.21 ± 1.26	20.09 ± 1.09
7	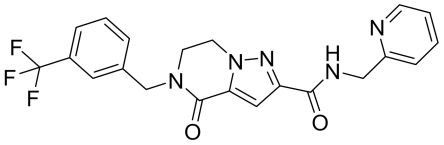	7.25 ± 2.32	15.03 ± 1.14	19.34 ± 2.05
8	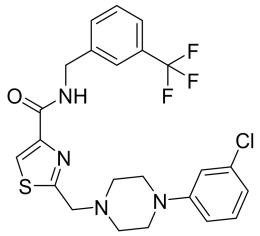	7.22 ± 1.20	18.22 ± 1.98	18.76 ± 2.03
9	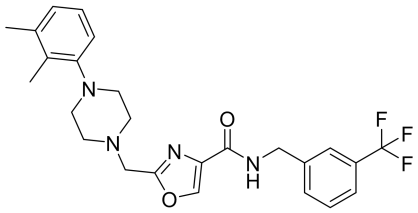	5.56 ± 1.01	11.09 ± 2.09	17.90 ± 1.90
10	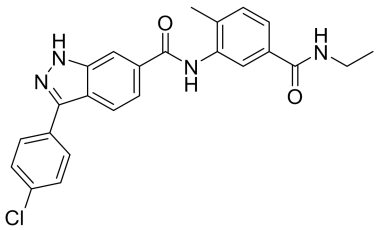	3.37 ± 0.24	8.21 ± 1.24	10.08 ± 2.11

2.4 Cell death pathway assay

To explore the cell death pathway of compound **10**, the cell survival rate was determined by co-treatment with several common inhibitors targeting different cell death pathways and compound **10**. Compound **10** was treated with apoptosis inhibitor Z-VAD-FMK, necrosis inhibitor Necro, iron chelator DFO, ferroptosis inhibitor Fer-1, copper chelator TTM and autophagy inhibitor 3-MA. The maximum concentration of

the corresponding inhibitors was selected to play a rescue effect without killing cells more effectively, which were 10 μM, 30 μM, 10 μM, 125 μM, 10 μM, 10 μM, and 50 μM, respectively. Results showed that compound **10** significantly inhibited cell viability. In the presence of 3-MA, cell viability increased from less than 50% to more than 80%. However, other death pathway inhibitors for rescuing cell death induced by compound **10** was almost invalid. It significantly indicated that autophagy inhibitor rescued the cell death induced by compound **10**, which indirectly indicated that compound **10** induced TNBC cell death through autophagy pathway (Figure 3).

Next, Western blot experiments were carried out for further verification. The level of autophagy was determined by the ratio of LC3-Ⅱ/Ⅰ. LC3-Ⅰ is formed by the cleavage of a polypeptide from the C-terminus of pro-LC3 by ATG4. When autophagy occurs, LC3-Ⅰ covalently binds to phosphatidylethanolamine under the action of ATG7 and ATG12-ATG5-ATG16L to form LC3-II, which binds to the autophagosome membrane [13]. Therefore, including autophagy can lead to the transformation of LC3-Ⅰ to LC3-Ⅱ. p62 is a widely studied autophagy substrate. The linker region (LRS) between the zinc finger and UBA domains of p62 protein is responsible for binding to autophagy receptor Atg8/LC3. During autophagosome formation, p62 acts as a bridge connecting LC3 to aggregated proteins and is selectively encapsulated into the autophagosome. It is then degraded by proteolytic enzymes in the autolysosome [14]. Therefore, the expression of p62 showed a negative correlation with autophagic activity. In the Figure 3B, it can be clearly seen that compound **10** downregulated p62 and induced the conversion of LC3-Ⅰ to LC3-Ⅱ, indicating that compound **10** induced canonical autophagy.

https://doi.org/10.55415/deep-2023-0056.v1

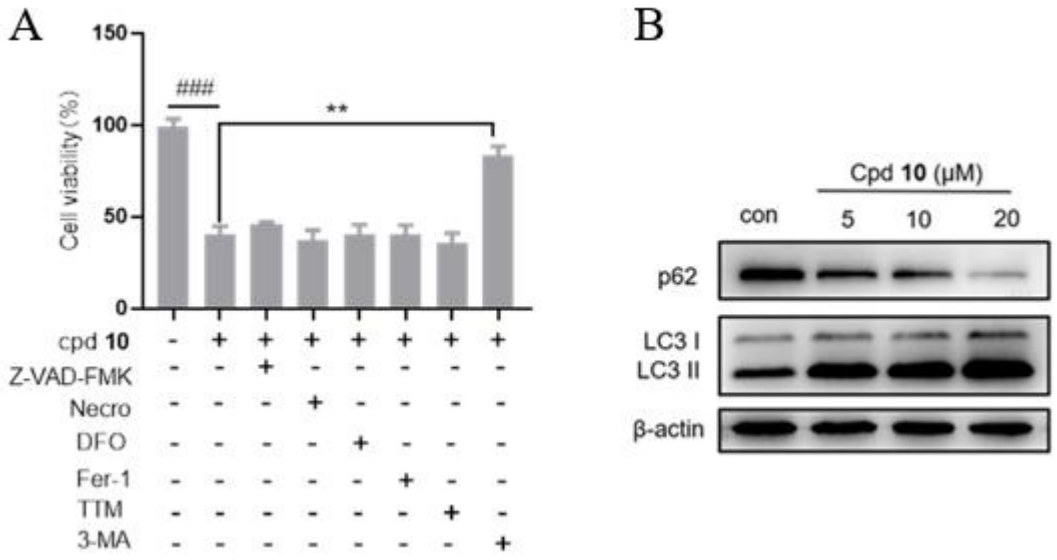

Figure 3. (A) Co-inhibition assay of compound **10** and six other death pathway inhibitors. (B) Western blot assay of cells treated with compound **10**.

Although compound **10** was successfully screened out as a p38α inhibitor with good inhibitory activity in this study, there are still many shortcomings, and further research and analysis are needed in the future. First, only MCDB, ACDB and SPECS databases are selected for virtual screening in this experiment, and the limitation of library selection restrict screening results. Second, only one docking application, Discovery Studio, was used for virtual screening, which is not excluded that the results may differ after virtual screening using other docking application. In recent years, the rapid development of AI technology and deep learning technology has also promoted virtual screening. In the future, we can consider further understanding how tools such as deep learning can be used to improve the accuracy of virtual screening. Third, only two types of triple-negative breast cancer cells were used for the anti-proliferation assay, and the samples size were relatively too small. In addition, there is a problem of inhibitor selection in exploring cell death pathway experiments. Whether the selected inhibitors of the typical cell death pathway were complete, whether other inhibitors could be more precise as inhibitors of the same death pathway, and whether the selected inhibitor interacted with compound **10** resulting in reduced inhibitory activity rather than competition for the substrate. Finally, further understanding of the role of p38α *in vivo* is needed to inform the design of its inhibitors. In addition, the

rapid development of precision medicine and biomedical technology in recent decades also provides infinite possibilities for its inhibitors in the future.

In summary, p38α is one of the most important members of the MAPK family and plays an important role in a variety of diseases such as neurodegenerative diseases, cancer, cardiovascular diseases and so on. Based on the structural characteristics of p38α, a multi-step structure-based virtual screening was carried out, and the most effective compound **10** was identified with an IC_{50} of 3.37 ± 0.24 μM on p38α. Compound **10** effectively inhibited the proliferation of MDA-MB-231 and MDA-MB-468 triple-negative breast cancer cells with IC_{50} values of 8.21 ± 1.24 μM and 10.08 ± 2.11 μM, respectively. Furthermore, we demonstrated that compound **10** causes cell death via autophagy pathway. Western blot further explored the autophagy pathway, and the results showed that compound **10** down-regulated the marker substrate p62 of autophagy and converted LC3-Ⅰ to LC3-Ⅱ. Our study provides more reference for the research of p38α-related therapy and the development of novel drugs targeting p38α.

Acknowledgements

This work was supported by grants from the National Natural Science Foundation of China (Grant 22177083), Sichuan Science and Technology Program (Grant 2022NSFSC1290), 1·3·5 project for disciplines of excellence–Clinical Research Incubation Project, West China Hospital, Sichuan University (ZYJC21016), and West China Nursing Discipline Development Special Fund Project, Sichuan University (Grant HXHL21011).

Conflict of interest

No conflicts of interest.

References

[1] Whitaker RH, Cook JG: Stress Relief Techniques: **p38 MAPK Determines the Balance of Cell Cycle and Apoptosis Pathways.** *Biomolecules* 2021, 11:1444.

[2] Weng J, Tu M, Wang P, Zhou X, Wang C, Wan X, Zhou Z, Wang L, Zheng X, Li J, Wang Z, Wang Z, Chen C: **Amiodarone induces cell proliferation and myofibroblast differentiation via ERK1/2 and p38 MAPK signaling in fibroblasts.** *Biomed Pharmacother* 2019, 115:108889.

[3] Wagner EF, Nebreda AR: **Signal integration by JNK and p38 MAPK pathways in cancer development.** *Nat Rev Cancer* 2009, 9:537-549.

[4] Engel FB, Schebesta M, Duong MT, Lu G, Ren S, Madwed JB, Jiang H, Wang Y, Keating MT: **p38 MAP kinase inhibition enables proliferation of adult mammalian cardiomyocytes.** *Genes Dev* 2005, 19:1175-1187.

[5] Hui L, Bakiri L, Mairhorfer A, Schweifer N, Haslinger C, Kenner L, Komnenovic V, Scheuch H, Beug H, Wagner EF: **p38alpha suppresses normal and cancer cell proliferation by antagonizing the JNK-c-Jun pathway.** *Nat Genet* 2007, 39:741-749.

[6] Ventura JJ, Tenbaum S, Perdiguero E, Huth M, Guerra C, Barbacid M, Pasparakis M, Nebreda AR: **p38alpha MAP kinase is essential in lung stem and progenitor cell proliferation and differentiation.** *Nat Genet* 2007, 39:750-758.

[7] Dolado I, Swat A, Ajenjo N, De Vita G, Cuadrado A, Nebreda AR: **p38alpha MAP kinase as a sensor of reactive oxygen species in tumorigenesis.** *Cancer Cell* 2007, 11: 191-205.

[8] Thornton TM, Rincon M: **Non-classical p38 map kinase functions: cell cycle checkpoints and survival.** *Int J Mol Sci* 2015, 5: 44-51.

[9] Batool M, Ahmad B, Choi S: **A Structure-Based Drug Discovery Paradigm.** *Int J Mol Sci* 2019, 20: 2783.

[10] Park H, Chien PN, Ryu SE: **Discovery of potent inhibitors of receptor protein tyrosine phosphatase sigma through the structure-based virtual screening.** *Bioorg Med Chem Lett* 2012, 22: 6333-6337.

[11] Gangwal RP, Damre MV, Das NR, Dhoke GV, Bhadauriya A, Varikoti RA, Sharma SS, Sangamwar AT: **Structure based virtual screening to identify selective phosphodiesterase 4B inhibitors.** *J Mol Graph Model* 2015, 57: 89-98.

[12] Antoon JW, Bratton MR, Guillot LM, Wadsworth S, Salvo VA, Elliott S, McLachlan JA, Burow ME: **Pharmacology and anti-tumor activity of RWJ67657, a novel inhibitor of p38 mitogen activated protein kinase.** *Am J Cancer Res* 2012, 2: 446-458.

[13] Zhang J, Wang G, Zhou Y, Chen Y, Ouyang L, Liu B: **Mechanisms of autophagy and relevant small-molecule compounds for targeted cancer therapy.** *Cell Mol Life Sci* 2018, 75:1803-1826.

[14] Bu F, Zhang J, Shuai W, Liu J, Sun Q, Ouyang L: **Repurposing drugs in autophagy for the treatment of cancer: From bench to bedside.** *Drug Discov Today* 2022, 27:1815-1831.

Graphic Abstract